Elastic Bounded Diffusion. Dynamics of Ferrocene-Labeled Poly(ethylene glycol) Chains Terminally Attached to the Outermost Monolayer of Successively Self-Assembled Monolayers of Immunoglobulins

Agnès Anne, Christophe Demaille, and Jacques Moiroux*

Contribution from the Laboratoire d'Electrochimie Moléculaire, Unité Mixte de Recherche Université−CNRS No 7591, Université de Paris 7, Denis Diderot, 2 place Jussieu, 75251 Paris Cedex 05, France

Received May 28, 1999

Abstract: A model of elastic bounded diffusion is presented for the quantitative analysis of the dynamics of redox probes borne by the loose ends of linear and flexible polymeric chains terminally grafted to building blocks of a self-assembled construction. Experimentally, poly(ethylene glycol) chains bearing a ferrocene probe were terminally attached at the last one of a series of immunoglobulins monolayers successively self-assembled on top of a glassy carbon electrode. In cyclic voltammetry, the creation of a concentration gradient provoked a diffusion-like displacement of the ferrocene probe counterbalanced by the springlike elasticity of the terminally attached polymeric chain. The morphology and the intensity of the signal depend markedly on the distance separating the terminal attachment from the electrode surface and on the potential scan rate. The observed changes are qualitatively and quantitatively justified by the model. Both the diffusion and the elasticity can be quantitatively characterized.

Introduction

New heterobifunctional poly(ethylene glycol) (PEG) derivatives have been synthesized recently.[1] Particularly, a linear NHS−PEG−Fc molecule is obtained when an *N*-hydroxysuccinimide (NHS) activated ester and a ferrocene (Fc) redox label are introduced at each end of the PEG chain.[1c] The activated NHS can be used for terminal attachment of the PEG chain to NH_2 bearing supports such as modified glassy carbon surfaces[2] or proteins.[3] The loose end of the linear chain bears the ferrocene redox label, which is small and only slightly solvent sensitive.[4] It can be used as an electrochemical probe in a transient technique such as cyclic voltammetry. When the electrode potential is positive enough to oxidize ferrocene, an electric current flows. Such a current results from the flux of ferrocene redox heads toward the electrode surface, and its intensity is a measure of this flux, which depends on the PEG chain dynamic flexibility. Therefore cyclic voltammetry of attached NHS−PEG−Fc provides a new approach for the quantitative analysis of the dynamics of terminally attached linear polymer chains.

In a recent work, NHS−PEG−Fc molecules of different molar weights were terminally attached to the surface of a glassy carbon electrode and the flexibility of the PEG chains was characterized quantitatively.[1c] The present report deals with another configuration. The redox labeled PEG chains were attached to a given immunoglobulin G (IgG). The latter was immobilized at the electrode surface in an ordered structure made of self-assembled and adequately chosen IgG's. That enabled us to control the distance separating the anchoring points of the polymer chains from the electrode surface.

The ordered immunological construction was built according to a procedure that has been well documented in the past few years.[5] It consists of a step-by-step immobilization of successive molecular monolayers of IgG's on top of an initial monolayer which is adsorbed at the electrode surface. More precisely, a first monolayer of antigen (an IgG of a given animal species A) is irreversibly adsorbed at the electrode surface. Taking advantage of the remarkable efficiency of antigen−antibody molecular recognition, the antigen is subsequently recognized by an antibody to IgG's of A raised specifically in another animal species B. The following monolayer is immobilized by recognition of the antibody produced in B by an anti-B antibody produced in A. The resulting outermost monolayer has therefore the same antigenic nature as the first immobilized (adsorbed) monolayer since it consists of immunoglobulins generated in A. Then, it can react anew with the anti-A antibody solution. The whole process is repeated until the desired number of successively immobilized monolayers is reached, routinely more than 10.[5c] The outstanding stability of the structures thus obtained has been well established.[5b−e] They can be easily endowed with a catalytic activity that is triggered and measured electrochemically provided that one of the antibodies involved in the construction is labeled with a redox enzyme.[5] Moreover

(1) (a) Anne, A. *Tetrahedron Lett.* **1998**, *39*, 561−564. (b) Anicet, N.; Anne, A.; Moiroux, J.; Savéant, J.-M. *J. Am. Chem. Soc.* **1998**, *120*, 7115−7116. (c) Anne, A.; Moiroux, J. *Macromolecules* **1999**, *32*, 5829.

(2) Anne, A.; Blanc, B.; Moiroux, J.; Savéant, J.-M. *Langmuir* **1998**, *14*, 2368−2371.

(3) Hermanson, G. T. *Bioconjugate Techniques*; Academic Press: San Diego, 1996; p 293.

(4) Hupp, J. T. *Inorg. Chem.* **1990**, *29*, 5010−5012.

(5) (a) Bourdillon, C.; Demaille, C.; Guéris, J.; Moiroux, J.; Savéant, J.-M. *J. Am. Chem. Soc.* **1993**, *115*, 12264−11269. (b) Bourdillon, C.; Demaille, C.; Moiroux, J.; Savéant, J.-M. *J. Am. Chem. Soc.* **1994**, *116*, 10328−10329. (c) Bourdillon, C.; Demaille, C.; Moiroux, J.; Savéant, J.-M. *J. Am. Chem. Soc.* **1995**, *117*, 11499−11506. (d) Bourdillon, C.; Demaille, C.; Moiroux, J.; Savéant, J.-M. *Acc. Chem. Res.* **1996**, *29*, 529−535. (e) Bourdillon, C.; Demaille, C.; Moiroux, J.; Savéant, J.-M. *J. Am. Chem. Soc.* **1999**, *121*, 2401−2408.

10.1021/ja991780i CCC: $18.00
Published on Web 10/23/1999

Chart 1

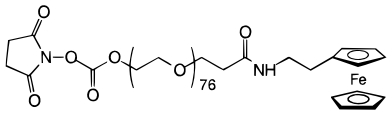

NHS-PEG-Fc

the enzyme spatial distribution can be controlled at will simply by choosing the proper sequence of building blocks in the step-by-step immunological immobilization.[5b−d] Similarly, in the study described hereafter, we aim at precisely anchoring the PEG−Fc chains within the self-assembled structure by making use of an IgG labeled with PEG−Fc chains as one of the building blocks.

It has been also shown that the high efficiency of the antigen−antibody reaction allows attaining the saturation of each monolayer under easily fulfilled practical conditions, the time of reaction and the amounts of reagents required being quite reasonable. At saturation, the surface concentration of antibody molecules immobilized in each monolayer corresponds to the maximum lateral compactness attainable. All the monolayers are therefore structurally identical.[5]

The average molar weight of the PEG chains used in all experiments is 3400; it corresponds to a degree of polymerization of 77 (see the Chart 1).

In a preliminary study, PEG−Fc chains, with no NHS activated end, were introduced in the surrounding aqueous solution and cyclic voltammetry was used to characterize quantitatively their free diffusion across the assembled protein structure.[6] When the PEG−Fc chains were terminally attached at various distances from the electrode surface, the observed electrochemical behavior could longer be accounted for by free diffusion. A type of bounded diffusion must be considered.[7] We develop an approach of the dynamics of the ferrocene heads of the terminally attached PEG chains, making allowance for both a diffusion contribution and an elastic penalty. The latter results from the effect of a springlike force which expresses that the further a ferrocene head moves away from its equilibrium position in the structure the slower the motion; the elasticity of the terminally attached PEG chain is thus involved. The fact that we were able to control the distance from the electrode surface at which the PEG−Fc chains were attached enabled us to elaborate and test a model of elastic bounded diffusion for the redox heads. Simulated cyclic voltammograms were derived from the model. They fit remarkably well the experimentally observed behavior and show that we are able to analyze quantitatively the dynamics of the terminally attached PEG chains quite satisfactorily.

Results and Discussion

Terminal Attachment of the PEG−Fc Chains to the IgG Self-Assembly. The IgG self-assemblies were constructed onto glassy carbon electrodes by successive immobilization of monolayers of polyclonal anti-goat mouse antibodies and anti-mouse goat antibodies, as described in the Experimental Section. A sketch of the resulting structure is given in Figure 1. It is worth emphasizing that the binding of each new monolayer relies on the molecular recognition of the outermost (*n*th) monolayer of the already assembled structure by antibodies which are introduced in solution. Eventually that will produce the ($n + 1$)th immobilized monolayer. Therefore, the antibodies

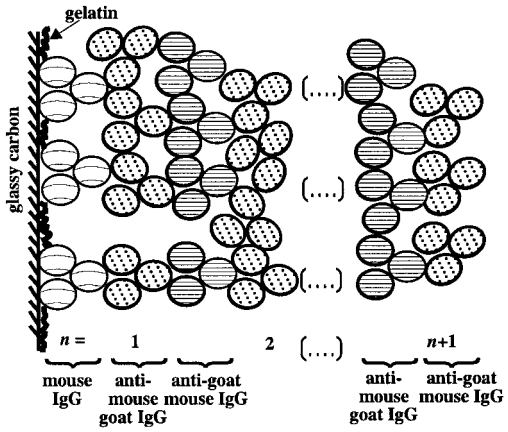

Figure 1. Sketch of the step-by-step immobilization of $n + 1$ successive monolayers of immunoglobulins.

are oriented within the assembly in such a way that their substructures, which are capable of molecular recognition, namely, their Fab subunits, are necessarily oriented toward the electrode. Gelatin was adsorbed at the glassy carbon surface to prevent nonspecific binding.

NHS−PEG−Fc chains were covalently grafted to an anti-goat IgG produced in mouse and to an anti-mouse IgG produced in goat through the reaction of the NHS activated ester with accessible amino groups of the immunoglobulins.[3] ICP-MS assays of iron in samples of derivatized Fc−PEG−IgG's showed that the degree of PEG−Fc labeling was reproducible. It was found to be 7 and 17 for the anti-mouse goat IgG and for the anti-goat mouse IgG, respectively.

When a glassy carbon disk electrode bearing an adsorbed layer of goat (or mouse) IgG is immersed in a solution containing PEG−Fc-labeled anti-goat (or anti-mouse) IgG's and transferred in the buffered solution after thorough washing, a cyclic voltammogram like the one reproduced in Figure 2a is recorded.

Such a cyclic voltammogram is typical of the behavior of the P/Q redox couple when both P and Q are confined near the electrode surface.[8] The corresponding structure is sketched in Figure 3b.

As expected for a P/Q surface-confined redox system exhibiting a Nernstian behavior, the peak heights are proportional to the potential scan rate (υ) as long as $\upsilon \leq 1$ V/s, the peak-to-peak separation is less than 5 mV, and the width of each peak at midpeak height is ~95 mV.[8] Whatever the electrode coverage or the degree of PEG−Fc IgG labeling, the apparent standard potential (E°_{PQ}) then measured is 155 ± 3 mV, a value in good agreement with the E°_{PQ} value of 149 ± 3 mV determined earlier with soluble PEG−Fc chains.[6] The amount of confined Fc is given by the area under one peak of the cyclic voltammogram. We found that it increased with the time of immersion in the Fc−PEG−IgG solution until a saturating value, which was reached after 48 h. Related to the geometric area of the disk electrode, the PEG−Fc surface concentration at saturation was $\Gamma^\circ = (2.8 \pm 0.3) \times 10^{-11}$ mol/cm^2 for the anti-mouse Fc−PEG−IgG and $\Gamma^\circ = (1.4 \pm 0.1) \times 10^{-11}$ mol/cm^2 for the anti-goat Fc−PEG−IgG. When the PEG−Fc coverage was converted into labeled Fc−PEG−IgG coverage,we found 4×10^{-12} mol/cm^2 for the anti-mouse IgG bearing 7 PEG−Fc chains and 0.82×10^{-12} mol/cm^2 for the anti-goat IgG bearing 17 PEG−

(6) Demaille, C.; Moiroux, J. *J. Phys. Chem.* (in press).

(7) Blauch, D. N.; Savéant, J.-M. *J. Am. Chem. Soc.* **1992**, *114*, 3323−3332.

(8) Laviron, E. Voltammetric Methods for the Study of Adsorbed Species. In *Electroanalytical Chemistry*; Bard, A. J., Ed.; Marcel Dekker: New York, 1982; Vol. 12, pp 53−157.

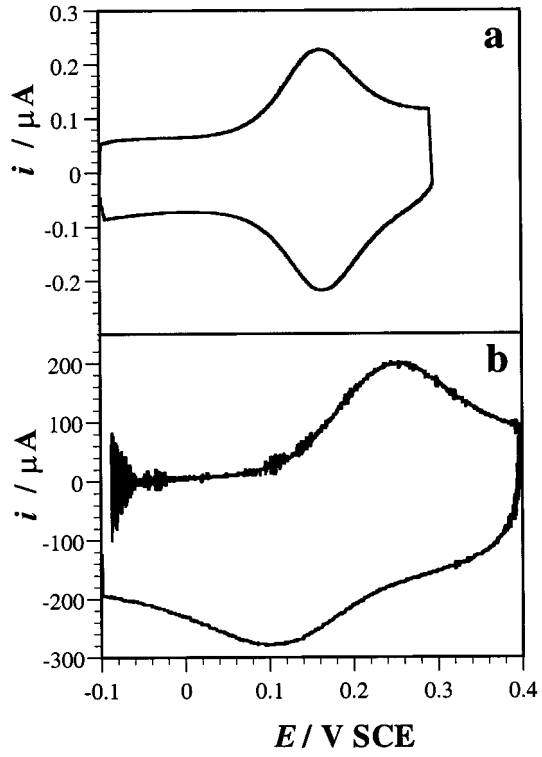

Figure 2. Cyclic voltammogram obtained with an electrode at which a monolayer of PEG−Fc-labeled polyclonal anti-mouse goat antibody is attached on top of an adsorbed monolayer of mouse IgG. PEG−Fc: 3-mm-diameter glassy carbon disk electrode, pH 8.0 phosphate buffer (0.1 M ionic strength). In (a), surface concentration $\Gamma^\circ = 2.8 \times 10^{-11}$ mol/cm^2 and potential scan rate $\upsilon = 0.1$ V/s. In (b), surface concentration $\Gamma^\circ = 2.4 \times 10^{-11}$ mol/cm^2 and potential scan rate $\upsilon = 200$ V/s with ohmic drop compensation.

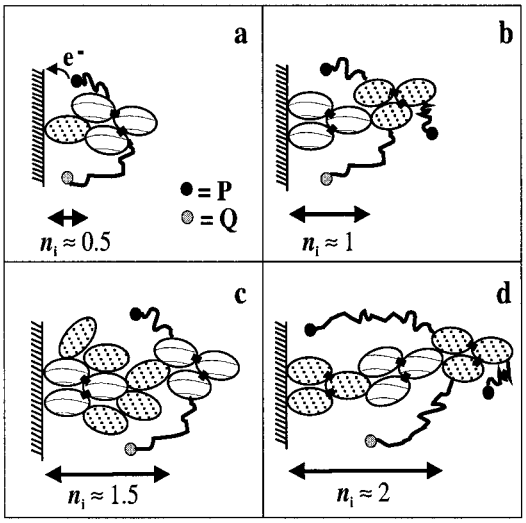

Figure 3. Sketch of the self-assemblies of immunoglobulin monolayers used for terminal attachment of PEG−Fc chains at various distances from the electrode surface. Dotted and hatched blobs indicate immunoglobulins produced in goat (anti-mouse) and mouse (anti-goat), respectively. A whole IgG is made of a regular triangle of three jointed blobs. Isolated dotted blobs represent Fab fragments of the polyclonal anti-mouse goat antibody. In (a), the Fab fragment is initially adsorbed at the glassy carbon electrode surface and is recognized by a PEG−Fc-derivatized anti-goat mouse whole antibody. In (b), the mouse whole IgG is adsorbed and recognized by a PEG−Fc-derivatized anti-mouse goat whole antibody. In c, the mouse whole IgG is adsorbed and recognized by the Fab fragment itself recognized by a PEG−Fc-derivatized anti-goat mouse whole antibody. In (d), only whole IgG's are self-assembled.

Fc chains. Considering the respective sizes of an IgG (∼15 nm)[9] and of a PEG−Fc chain (end-to-end distance of the PEG coil = Flory radius = R_F = 5 nm),[10] the lesser coverage obtained with the IgG bearing 17 PEG−Fc chains is a consequence of its greater bulkiness since the saturation is reached at full lateral compactness. The preceding results also show that, despite PEG−Fc labeling, the specific avidity of the Fc−PEG−IgG antibody toward the antigen is maintained. The irreversibility of the binding is ascertained by the outstanding persistence of the electrochemically assayed ferrocene coverage of the modified electrodes; less than 10% is lost in four weeks.

Effect of the Distance Separating the Terminal Attachment of the PEG−Fc Chains from the Electrode Surface. At high potential scan rates, the cyclic voltammogram of an electrode bearing one Fc−PEG−IgG monolayer ceases giving rise to symmetrical signals. In Figure 2b, the potentials of the anodic and cathodic peaks are no longer identical and both peaks are broad because the redox probes need a time, which becomes a limiting factor, to diffuse toward the electrode surface. A diffusion layer having a size similar to the IgG coating thickness develops within the film. The voltammetric signals then depend on the dynamics of the PEG−Fc chains.

A fundamental parameter is the distance separating the terminal attachment of the chains from the electrode surface. The step-by-step technique used for the construction of the ordered IgG structure allows us to modulate this parameter simply by changing the thickness of the IgG assembly onto which the Fc−PEG−IgG monolayer is finally immobilized. This thickness can be controlled either by varying the number of underlying IgG monolayers or by using smaller building blocks made of Fab fragments. Such fragments of IgG's are endowed with the same specific affinity, concerning molecular recognition, as the whole IgG molecule but are ∼2 times smaller.[9] Therefore, constructions have been assembled according to the scheme described in Figure 3, each one positioning the Fc−PEG−IgG monolayer at a different distance away from the electrode surface. The distance is proportional to the number n_i of protein monolayers intercalated between the electrode and the Fc−PEG−IgG layer, a monolayer of whole IgG counting for 1 and a Fab monolayer counting for 0.5 in the sum giving n_i.

At low enough potential scan rates, when the ferrocene head motion is not rate limiting, cyclic voltammograms similar to the one reproduced in Figure 2 were always recorded whatever $n_i \leq 2$. For $n_i > 2$, the distance separating the terminal attachment of the PEG−Fc chain from the electrode surface probably exceeds the length of the fully extended chain of 77 monomer units, which is ∼25 nm. The symmetrical cyclic voltammograms enable us to determine the total PEG−Fc coverage. Moreover, all the voltammograms are centered around the same standard potential, a result indicating that the Fc probes do not interact and have the same environment as in solution.

At each n_i, the morphological change observed in the presence of only one intercalating IgG monolayer ($n_i = 1$, see Figure 2b) always occurs when the potential scan rate is raised. However, the υ region in which it takes place may differ by several orders of magnitude depending on n_i ($0.5 \leq n_i \leq 2$). The greater the n_i the earlier the transition. The anodic and

(9) Lamy, J.; Lamy J.; Billiald, P.; Sizaret, P. Y.; Cavé, G.; Frank, J.; Motta, G. *Biochemistry* **1985**, *24*, 5532−5542.

(10) Vincent, B.; Luckham, P.; Waite, F. A. *J. Colloid Interface Sci.* **1980**, *73*, 508−521.

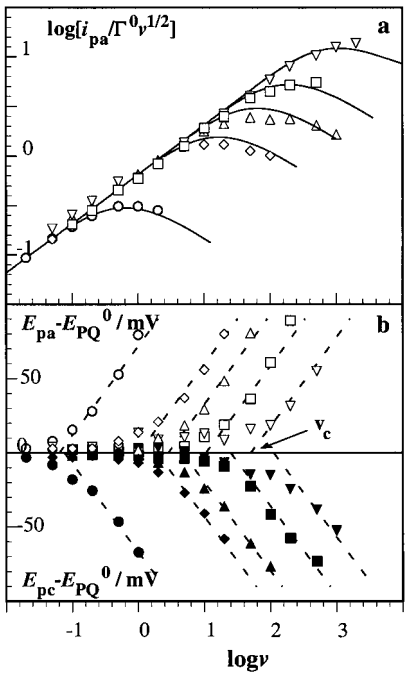

Figure 4. Cyclic voltammetry of the ferrocene heads of PEG−Fc chains terminally attached at various distances from the electrode surface. Experimental data. Potential scan rate (v) dependence of (a) the anodic peak current (i_{pa}) and (b) the anodic and cathodic peak potentials (E_{pa} and E_{pc}, respectively, the latter in black symbols). The greater the n_i, the higher the distance from the electrode surface (see text), $n_i = 0.5$ (▽), 1 (□), 1.25 (△), 1.5 (◇), 2 (○). In (a), the continuous curves are computed taking λ ($\lambda = x_e(k_{spr}/2RT)^{1/2}$; see text) = 1.26, 1.89, 2.19, 2.52, and 3.14 for $n_i = 0.5$, 1, 1.25, 1.5, and 2, respectively. In (b), the absolute value of the slope of all the dashed straight lines is 60 mV.

cathodic peak potentials E_{pa} and E_{pc}, respectively, and the anodic peak current (i_{pa}) function $i_{pa}/\Gamma^\circ v^{1/2}$ are plotted versus log(v) in Figure 4 for electrodes bearing IgG assemblies with different n_i's. To make the comparison more explicit, the current is normalized vis à vis the surface concentration Γ° of attached PEG−Fc. Figure 4a shows that $i_{pa}/\Gamma^\circ v^{1/2}$ increases linearly with log(v) until it reaches a plateau whose height depends markedly on n_i. Figure 4b shows that, above a critical scan rate v_c, E_{pa} and E_{pc} shift linearly away from E°_Q with a slope of 60 mV per v decade. Increasing or decreasing n_i only results in displacing the region of linear variation toward lower or higher potential scan rates, respectively. The dramatic changes in peak characteristics caused by changes in the anchoring distance of the PEG−Fc chains cannot be accounted for by free diffusion of the Fc probes. A model allowing for quantitative analysis of the dynamics of terminally attached PEG−Fc chains must be elaborated.

Model of Elastic Bounded Diffusion. A model of bounded diffusion was elaborated previously to describe electron percolation in redox polymers.[7] In that model, each redox site was attached to its own anchoring point in the structure by an imaginary spring. The conduction of electrons throughout the film did not result from the bounded diffusion of the redox centers alone; it involved necessarily electron hopping between the redox sites of the successive layers. Charge transport resulting from the sole physical displacement of the redox sites through bounded diffusion was not permitted. In the present case, we need a model that describes the transient dynamics of a single layer of redox centers, the extent of their physical displacement being sufficient to reach the electrode surface.

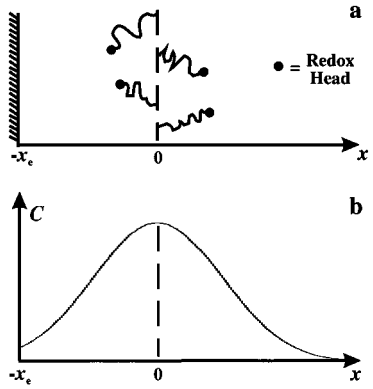

Figure 5. Equilibrium spatial distribution of the ferrocene heads of PEG−Fc chains terminally attached to a monolayer of antibodies immobilized at a given distance from the electrode surface.

In the absence of external force, the ferrocene heads borne by the elastic PEG chains would lie at rest at an average distance from the electrode surface which would practically coincide with the average distance of the anchoring points of the terminally attached PEG chains, i.e., the distance at which the Fc−PEG−IgG monolayer is immobilized.

The chains can extend toward the electrode until their ferrocene heads reach the electrode surface and toward the solution up to a limit corresponding to the length of the fully stretched chain L_{fs}. We are interested only in the motion of the ferrocene heads perpendicularly to the electrode surface. We assume that the elasticity of the PEG chain can be mimicked by an harmonic oscillator, and then the springlike force F_{spr} that tends to bring back the ferrocene head to its resting position is $F_{spr} = -k_{spr}x$, k_{spr} being a spring constant and x measuring the spring elongation away from the resting position of the ferrocene head as indicated in Figure 5. The existence of a concentration gradient gives rise to an osmotic force $F_{os} = -(k_BT/C)(\partial C/\partial x)$, with k_B the Boltzmann constant and C the ferrocene volume concentration at any x and time t. When the Fc head moves a drag force $F_{dr} = -k_{dr}V$ must be overcome, with k_{dr} the corresponding drag coefficient and V the velocity of the Fc head. At the time scale of molecular motion, the ferrocene head reaches a stationary velocity V_l and

$$\frac{k_BT}{C}\frac{\partial C}{\partial x} + k_{spr}x + k_{dr}V_1 = 0$$

The flux $J_{x,t}$ of Fc at time t through the plane located at distance x is given by $J_{x,t} = CV_l$, and the above equation leads to the following expression for the flux under conditions of elastic bounded diffusion:

$$J_{x,t} = -\frac{k_BT}{k_{dr}}\frac{\partial C}{\partial x} - \frac{k_{spr}}{k_{dr}}Cx = -D\left(\frac{\partial C}{\partial x} + \frac{k_{spr}}{RT}Cx\right)$$

the diffusion coefficient D being related to the drag coefficient by the Einstein relation ($D = k_BT/k_{dr}$), and the spring constant k_{spr} being then defined as a molar quantity.

The second Fick law ($\partial C/\partial t = -\partial J_{x,t}/\partial x$) gives the following differential equation, which expresses the dynamics of the ferrocene heads in terms of their time- and space-dependent volume concentration:

$$\frac{\partial C}{\partial t} = D\left\{\frac{\partial^2 C}{\partial x^2} + \frac{k_{spr}}{RT}\frac{\partial (Cx)}{\partial x}\right\} \qquad (1)$$

A similar equation was previously established for the study of transient kinetics in chemical reactions implying bounded diffusion perpendicular to the reaction coordinate.[11]

At equilibrium, $J_{x,t} = 0$ and $\partial C/\partial t = 0$ whatever x and t. Taking into account that at $x = 0$, $J_{0,t} = -D(\partial C/\partial x)_{0,t}$, and introducing $C^* = C_{x=0}$, integration then leads to

$$C = C^* \exp(-k_{spr}x^2/2RT) \tag{2}$$

Equation 2 shows that, according to the present theoretical approach, the concentration profile of the ferrocene heads is given, at equilibrium, by a Gaussian distribution reproduced in Figure 5b.

The measured surface concentration Γ° is related to C by $\Gamma_0 = \int_{-x_e}^{L_{fs}} C\,dx$, x_e being the average distance at which the chains are terminally attached as shown in Figure 5a. Thus:

$$C^* = \frac{\Gamma^0\sqrt{2k_{spr}/\pi RT}}{\mathrm{erf}(L_{fs}\sqrt{k_{spr}/2RT}) + \mathrm{erf}(x_e\sqrt{k_{spr}/2RT})}$$

In cyclic voltammetry, the initial potential E_i is chosen to ensure that all the ferrocene heads exist in their reduced form P; therefore, the initial concentration profile of P is the Gaussian-shaped equilibrium concentration profile described above and $C_P = C_P^* \exp(-k_{spr}x^2/2RT)$. When the potential is scanned and becomes positive enough to convert a P head that reaches the electrode surface into its oxidized form Q, a current i is recorded in consequence. Surely the electron transfer is rapid compared to the chain mobility. The ratio $C_{P,-xe}/C_{Q,-xe}$ of the volume concentrations of P and Q at the electrode surface is then related to the electrode potential E by the Nersnt law: $C_{P,-xe}/C_{Q,-xe} = \exp[-(F/RT)(E - E^\circ_Q)]$.

The following changes in variables and parameters lead to a dimensionless formulation of the problem.

$$\tau = (F\upsilon/RT)t; \quad y = x(F\upsilon/RTD)^{1/2}; \quad \mu = x_e(F\upsilon/RTD)^{1/2};$$
$$l = L_{fs}(F\upsilon/RTD)^{1/2}; \quad p = C_P/C^*; \quad q = C_Q/C^*$$

and

$$\xi = (F/RT)(E - E^\circ_Q)$$

The Nernst equation becomes $p_{-\mu} = q_{-\mu}\exp(-\xi)$. The dimensionless current is $\psi = i/((FS\Gamma^0/RT)\sqrt{2FDk_{spr}\nu/\pi})$, S being the electrode surface geometric area.

The set of partial differential equations describing the dynamics of the ferrocene heads is

$$\begin{cases} \dfrac{\partial p}{\partial \tau} = \dfrac{\partial^2 p}{\partial y^2} + \beta\,\dfrac{\partial(yp)}{\partial y} \\ \dfrac{\partial q}{\partial \tau} = \dfrac{\partial^2 q}{\partial y^2} + \beta\,\dfrac{\partial(yq)}{\partial y} \end{cases} \tag{3}$$

The dimensionless parameter $\beta = k_{spr}D/F\upsilon$ compares the experimental observation time $RT/F\upsilon$ to the characteristic chain motion time $RT/k_{spr}D$. It is also convenient to introduce the dimensionless length $\lambda = x_e(k_{spr}/2RT)^{1/2}$, which compares the distance separating the resting plane from the electrode to a spring-related length $(2RT/k_{spr})^{1/2}$. Similarly the dimensionless length $\lambda_{fs} = L_{fs}(k_{spr}/2RT)^{1/2}$ compares the chain length at full extension to the spring-related length. The requirement that the redox heads can reach the electrode surface implies that $\lambda_{fs} > \lambda$.

The initial and boundary conditions are

$$\tau = 0,\ l > y > -\mu: \qquad p = \exp(-\beta y^2/2), \quad q = 0$$

$$y = -\mu,\ \tau \geq 0:$$
$$\psi[\mathrm{erf}(\lambda) + \mathrm{erf}(\lambda_{fs})] = (\partial p/\partial y)_{-\mu} - \beta\mu p_{-\mu}$$
$$= -(\partial q/\partial y)_{-\mu} + \beta\mu q_{-\mu}$$

$$y = l,\ \tau \geq 0: \quad (\partial p/\partial y)_l + \beta\mu p_l = (\partial q/\partial y)_l + \beta\mu q_l = 0$$

The dynamics of a chain does not depend on whether it bears a P or a Q head; thus, $p + q = \exp(-\beta y^2/2)$ whatever y. Particularly at $y = -\mu$ that implies

$$p_{-\mu} = \exp(-\lambda^2)\,\frac{\exp(-\xi)}{1 + \exp(-\xi)} \qquad \text{and}$$
$$q_{-\mu} = \frac{\exp(-\lambda^2)}{1 + \exp(-\xi)}$$

and only one in the set of two differential equations (3) need be solved.

Analytical solutions can be derived for several limiting situations described below.

***β* → ∞.** The potential scan rate is slow enough, or equivalently the chain motion fast enough, to allow the PEG chains to be permanently at equilibrium and $p = p_{-\mu}\exp[(\beta/2)(\mu^2 - y^2)]$. The current does not contain any information relative to the chain dynamics; it simply reflects the change in the overall surface coverage of P molecules that takes place as they are oxidized.

At $\tau = 0$, the dimensionless surface coverage γ_0 of ferrocene molecules is

$$\gamma_0 = \int_{-\mu}^{l} p_{\tau=0}\,dy = \int_{-\mu}^{l} \exp\left(-\frac{\beta}{2}y^2\right)dy$$
$$= \sqrt{\frac{\pi}{2\beta}}[\mathrm{erf}(\lambda) + \mathrm{erf}(\lambda_{fs})]$$

At each potential, the dimensionless surface γ_p coverage of ferrocene molecules in their P form is given by

$$\gamma_p = \int_{-\mu}^{l} p\,dy = \gamma_0 p_{-\mu}\exp(\lambda^2) = \gamma_0\,\frac{\exp(-\xi)}{1 + \exp(-\xi)}$$

The dimensionless current is

$$\psi = -\frac{1}{\gamma_0}\sqrt{\frac{\pi}{2\beta}}\frac{\partial\gamma_p}{\partial\xi} = \sqrt{\frac{\pi}{2\beta}}\,\frac{\exp(-\xi)}{[1 + \exp(-\xi)]^2}$$

and the corresponding anodic current is

$$i = \frac{F^2S\Gamma^\circ\nu}{RT}\,\frac{\exp[-(F/RT)(E - E^0_{PQ})]}{\{1 + \exp[-(F/RT)(E - E^0_{PQ})]\}^2}$$

This expression is identical to the one corresponding to the Nernstian behavior of a redox species such as P adsorbed at the electrode surface, as already mentioned.[8]

***β* → 0.** In that case, the time window of the experimental observation is so narrow that only the Fc heads located very close to the electrode surface are given time to move toward

(11) Agmon, N.; Hopfield, J. J. *J. Phys. Chem.* **1983**, *78*, 6947−6959. (erratum) Agmon, N.; Hopfield, J. J. *J. Phys. Chem.* **1984**, *80*, 592.

the surface. The set of differential equations (3) then reduces to the Fick second law for simple diffusion. This peculiar situation means that, no matter the spring strength or the position of the resting plane, the ferrocene heads dynamics can, at high enough scan rate, be described in terms of simple diffusion. A typical reversible and diffusion-controlled cyclic voltammogram is therefore predicted. However, as the initial concentration to consider then is the concentration $p = \exp(-\lambda^2)$ at the immediate vicinity of the electrode, the dimensionless peak current ψ_p tends toward

$$\psi_p = 0.446 \frac{\exp(-\lambda^2)}{\mathrm{erf}(\lambda) + \mathrm{erf}(\lambda_{fs})}$$

and the anodic peak current will tend toward

$$i_{p,a} = 0.446FS\sqrt{\frac{FDv}{RT}} \frac{\Gamma^\circ\sqrt{2k_{spr}/\pi RT}}{\mathrm{erf}(x_e\sqrt{k_{spr}/2RT}) + \mathrm{erf}(L_{fs}\sqrt{k_{spr}/2RT})} \times \exp\left(-\frac{k_{spr}}{2RT}x_e^2\right)$$

The above expression shows that the peak current is then proportional to the square root of v. Most of all, it also predicts that increasing the distance x_e of attachment will cause a marked decrease in the diffusion-controlled peak current recorded at sufficiently high potential scan rate in cyclic voltammetry for a Nernstian redox couple.

$\lambda \rightarrow 0$. Formally the system behaves as if the resting plane of ferrocene heads was located at the electrode surface. At low v an adsorption-like cyclic voltammogram such as the one described above for $\beta \rightarrow \infty$ is predicted. At high v, a reversible diffusion voltammogram is expected, as described above for $\beta \rightarrow 0$, the anodic peak current being then

$$i_{p,a} = 0.446FS\sqrt{\frac{FDv}{RT}} \frac{\Gamma^\circ\sqrt{2k_{spr}/\pi RT}}{\mathrm{erf}(L_{fs}\sqrt{k_{spr}/2RT})}$$

which is identical to the expression obtained for a Nernstian peak current resulting from the diffusion-controlled oxidation of a redox species present initially in the whole coating structure at an apparent and homogeneous concentration C_{app} given by

$$C_{app} = \Gamma^\circ \frac{\sqrt{2k_{spr}/\pi RT}}{\mathrm{erf}(L_{fs}\sqrt{k_{spr}/2RT})}$$

Thus, at both extremes of the v range, the behavior is similar to that of a film coating the electrode and containing freely diffusing redox molecules.[8] The concentration of redox sites within the film would be Γ°/ϵ, with ϵ the thickness of this equivalent homogeneous film. That shows that the voltammetric behavior of redox species submitted to elastic bounded diffusion, with a resting plane located at the electrode surface, is indistinguishable from the behavior of freely diffusing molecules trapped within a film having an equivalent thickness ϵ of

$$\epsilon = \sqrt{\pi RT/2k_{spr}}\,\mathrm{erf}(L_{fs}\sqrt{k_{spr}/2RT})$$

In the thin-film model, cyclic voltammetry gives access to the global parameter $\epsilon/(D)^{1/2} = (\pi RT/2k_{spr}D)^{1/2}\ \mathrm{erf}[L_{fs}(k_{spr}/2RT)^{1/2}]$ as already mentioned in a previous paper.[1c]

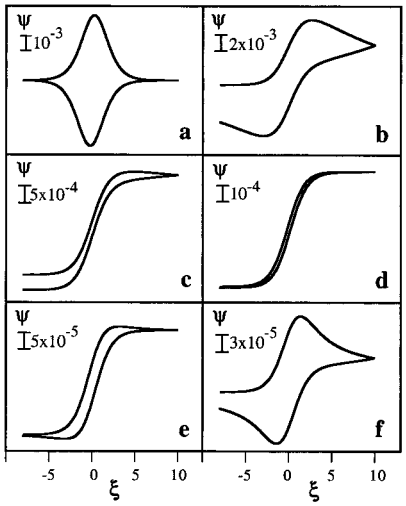

Figure 6. Cyclic voltammetry of the ferrocene heads of PEG−Fc chains terminally attached at a given distance from the electrode surface ($\lambda = x_e(k_{spr}/2RT)^{1/2} = 2.75$). Influence of the dimensionless parameter β on the computed dimensionless cyclic voltammogram, ψ versus ξ (see text). $\beta = k_{spr}D/Fv$ compares the experimental observation time RT/Fv to the characteristic chain motion time $RT/k_{spr}D$ (see text). $\beta =$ 5000, 100, 10, 0.5, 0.1, and 0.0001 in (a−f), respectively.

In the general case, the set of differential equations (3) can be solved numerically as described in Supporting Information. Simulations allow the computation of cyclic voltammograms for any values of the parameters β, λ, and λ_{fs}. They lead to the limiting cases described above. They also indicate that the voltammograms do not depend appreciably on λ_{fs} provided that $\lambda_{fs} > 2.5$, a condition that is always fulfilled.[12] Then only β and λ are required for the computation of the dimensionless voltammograms. That means that the Fc heads' concentration profile is controlled by the PEG chain elasticity rather than by the length of the fully stretched chain.

Cyclic voltammograms calculated for $\lambda = 2.75$ and various values of β are gathered in Figure 6. They illustrate clearly the morphological changes the signals should undergo as β decreases. At high β (i.e., low v), the cyclic voltammogram has the symmetrical shape corresponding to the limiting case $\beta \rightarrow \infty$. That corresponds to a location in zone A of the zone diagram drawn in Figure 7.

The peak separation increases with decreasing β until the voltammogram resembles a diffusion-controlled voltammogram (Figure 6b and general case in Figure 7). However, the peaks are broad and the cathodic peak is broader than the anodic one. As β decreases further, the peaks disappear and the voltammogram becomes almost plateau shaped (Figure 6c), with little or no hysteresis between the forward and backward scan (Figure 6d and zone K in Figure 7). Further decrease in β first results in hysteresis reappearance (Figure 6e back to the general case in Figure 7) and, at very low β (high v), the cyclic voltammogram is fully reversible and diffusion controlled as expected for $\beta \rightarrow 0$ (zone D in Figure 7).

The signal is plateau shaped when either x_e or k_{spr} is so large that most of the redox heads stay gathered in the resting plane during the potential scan. Then the concentration at the resting plane, which is the center of the Gaussian distribution at equilibrium, remains roughly constant ($p_{y=0} = 1$). Only a low, stationary, flux of redox heads leaves the resting plane toward

(12) (a) Pincus, P. *Macromolecules* **1976**, *9*, 386−388. (b) de Gennes, P. G. *Scaling Concepts in Polymer Physics*; Cornell University Press: Ithaca, NY, 1991; pp 29−53.

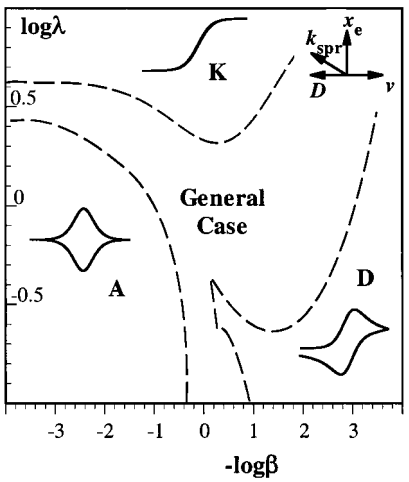

Figure 7. Cyclic voltammetry of the ferrocene heads of PEG−Fc chains terminally attached at a various distances from the electrode surface. Zone diagram showing the dependence of the computed cyclic voltammograms on the dimensionless parameters $\beta = k_{spr}D/Fv$ and $\lambda = x_e(k_{spr}/2RT)^{1/2}$, i.e., on the actual parameters D, k_{spr}, x_e, and v defined in the text. Zone A: adsorption-like behavior. Zone D: diffusion-controlled behavior. Zone K: plateau-shaped voltammogram with no hysteresis between the forward and reverse potential sweeps. Inside the dashed frontiers of the A, D, and K zones, the anodic peak (or plateau) current differs by less than 3% from the value corresponding to the limiting situation that characterizes the zone.

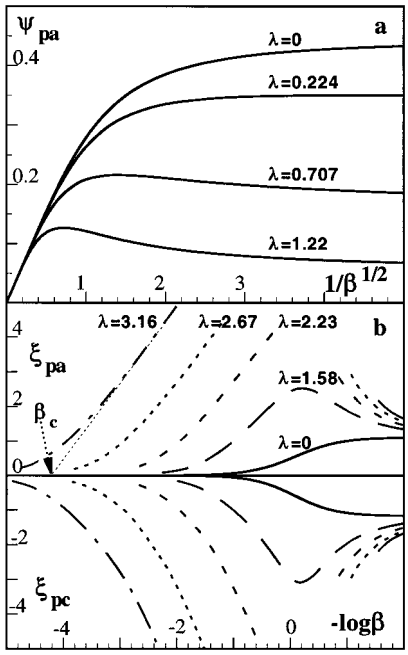

Figure 8. Cyclic voltammetry of the ferrocene heads of PEG−Fc chains terminally attached at a various distances from the electrode surface. Computed β dependence ($\beta = k_{spr}D/Fv$) of the dimensionless anodic peak current (ψ_{pa}) and peak potentials (anodic ξ_{pa}, cathodic ξ_{pc}).

the electrode. At any y, the corresponding dimensionless flux is $-(\partial p/\partial y) - \beta y p$. Integration between the resting plane ($y = 0$, $p = 1$) and the electrode surface ($y = -\mu$, $p = p_{-\mu}$) leads to a dimensionless current

$$\psi_{SS} = \frac{1}{1 + \exp(-\xi)} \sqrt{\frac{\beta}{2}} \{[1 + \mathrm{erf}(\lambda)] \int_0^{\lambda} \exp(y^2)\, dy\}^{-1}$$

and an actual current

$$i = \frac{FS\Gamma^{\circ}k_{spr}D}{RT\sqrt{\pi}} \{[1 + \exp(\lambda)] \int_0^{\lambda} \exp(y^2)\, dy\}^{-1} \times \frac{1}{1 + \exp\left[-\frac{F}{RT}(E - E^{\circ}_{PQ})\right]}$$

which is v independent. Besides, the half-wave potential is E°_{Q}.

Figure 6 also shows that a marked decrease in the dimensionless current accompanies the morphological changes. It is worth emphasizing that the cyclic voltammograms that may be controlled by elastic bounded diffusion go through all the morphological changes described in Figure 6 only for high enough values of λ. The zone diagram in Figure 7 shows that the voltammograms will remain peak shaped throughout the whole β range at small λ. The calculated variations of the dimensionless peak currents and potentials with β are plotted in Figure 8 for various λ. The peak potentials can only be measured when the signals are not plateau shaped.

Increasing v, i.e., decreasing β, the dimensionless peak current is initially proportional to $1/\beta^{1/2}$, a result implying that the actual anodic peak current is proportional to the potential scan rate.

The cyclic voltammogram is then typically adsorption-like ($\beta \rightarrow \infty$) and does not depend on λ. At low β (high v), the limiting situation corresponding to ($\beta \rightarrow 0$) is reached smoothly. The voltammogram does not depend any longer on β; the peak current is proportional to $v^{1/2}$ and decreases markedly with increasing λ. Between the two limiting situations, at each λ, the dimensionless peak current exhibits a maximum which is never observed when simple diffusion takes place within thin films ($\lambda = 0$).

With decreasing β, the forward and backward peak potentials initially shift away from E°_{Q} in opposite directions (Figure 8b). For λ high enough, the slope ($d\xi/d\log(\beta)$) of this initial shift reaches a constant value of 2.3. That implies a linear shift of 60 mV/decade of v for the actual peak potentials. An increase in λ causes a shift of the linear shift toward regions of higher β, i.e., lower v. The value of β_c, which depends only on λ and is defined as indicated in Figure 8b, characterizes the position of the linear peak potential shift on the log(β) scale. Simulations show that, at small λ, the shifts of the anodic and cathodic peak potentials are symmetrical. However, as λ increases, the exact value of the cathodic (reverse) peak potential starts to depend on the inversion potential ξ_f. Whatever λ, at low enough β the peaks shift back toward one another, and when $\beta \rightarrow 0$, the dimensionless anodic and cathodic peak potentials are 1.1 and −1.1, respectively, as expected for a diffusion-controlled reversible cyclic voltammogram.[13]

Quantitative Analysis of the Dynamics of Terminally Attached PEG−Fc Chains. It can be assumed that the resting plane of Fc heads is at the level of the outermost IgG monolayer, which is made of Fc−PEG−IgG's. To take into account the fact that the chains are probably grafted all around the ferrocene-labeled IgG's, we assume that the resting plane is located in the middle of the Fc−PEG−IgG monolayer. The distance between this imaginary resting plane and the electrode surface for a construction made of n_i IgG (or Fab) monolayers intercalated between the Fc−PEG−IgG layer and the electrode surface is thus taken as $x_e = (0.5 + n_i)l$ in the following, l being

(13) Andrieux, C. P.; Savéant, J.-M., Electrochemical reactions. In *Investigations of Rates and Mechanisms of Reactions, Techniques in Chemistry*; Bernasconi, C., Ed.; Wiley: New York, 1986; Vol. 6, 4/E, Part 2, pp 305−390.

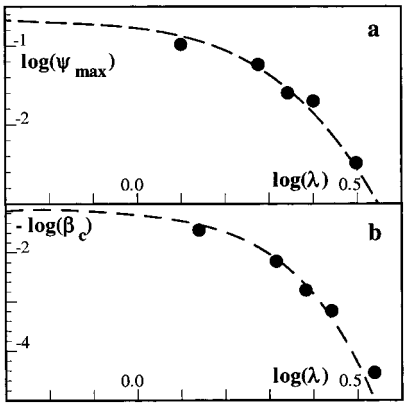

Figure 9. Cyclic voltammetry of the ferrocene heads of PEG−Fc chains terminally attached at various distances from the electrode surface. Starting from the left, the experimental data points (black circles) correspond to $n_i = 0.5$, 1, 1.25, 1.5, and 2. (a) Adjustment of the computed $\log(\psi_{max})$ vs $\log(\lambda)$ curve to the $\log(i_{pa}/\Gamma^0 v^{1/2})_{max}$ vs $\log(x_e)$ plot of experimental data (see text). The best fit is obtained for $k_{spr}D = 2.2 \times 10^8$ W/mol and $l\ k_{spr}^{1/2} = 89$ (J/mol)$^{1/2}$. (b) Adjustment of the computed $\log(\beta_c)$ vs $\log(\lambda)$ curve to the $\log(v_c)$ vs $\log(x_e)$ plot of experimental data (see text). The best fit is then obtained for $k_{spr}D = 1.7 \times 10^8$ W/mol and $lk_{spr}^{1/2} = 97$ (J/mol)$^{1/2}$.

the average distance separating the midplanes of two successively immobilized IgG monolayers.

Qualitatively the conclusions that can be drawn from the model of elastic bounded diffusion we elaborated are in very good agreement with the essential features of the experimental investigation. Particularly, the model justifies the sharp decrease in the $i_{pa}/\Gamma^\circ v^{1/2}$ ratio which can be caused by an increase in the distance separating the Fc−PEG−IgG monolayer and the electrode surface. It also accounts for the linear dependence of the peak potentials on v (60 mV/decade of v) and its characteristic shift to regions of lower potential scan rates that was observed when the Fc−PEG−IgG monolayer/electrode distance was increased (see Figures 4b and 8b). Experimentally such remarkable changes cannot be missed and they were also quantitatively analyzed.

The first type of fit between the computed and experimental data that we carried out concerned the dependence of $i_{pa}/\Gamma^\circ v^{1/2}$ on v (Figure 4a), which should accompany morphological changes in the signals; peaks should give way to plateau shaped currents and peaks again with increasing v. The upper limit of potential scan rate at which a peak current can be measured reliably results from the interference of the background current. The latter is mostly capacitive and proportional to v while the faradaic current we are interested in increases, at best, proportionally to $v^{1/2}$ in the high scan rate region and the signal-to-noise ratio may become very poor. This experimental limitation impedes the exploration of the $\beta \rightarrow 0$ limiting case for which the $i_{pa}/\Gamma^\circ v^{1/2}$ ratio is predicted to be v independent and the signal a peak anew. A decrease of $i_{pa}/\Gamma^\circ v^{1/2}$ with increasing v was observed only in a few cases (Figure 4a). However, the maximum of $i_{pa}/\Gamma^\circ v^{1/2}$ was always observed, a plateaulike current being recorded then. It corresponds to the theoretically predicted maximum value of the dimensionless current ψ_{max}, which depends only on λ. The $\log(\psi_{max})$ vs $\log(\lambda)$ plot is given in Figure 9a.

Adjustment of the experimental $\log(i_{pa}/\Gamma^\circ v^{1/2})_{max}$ vs $\log(x_e)$ plot to the theoretical one could be performed unequivocally only if x_e and $(i_{pa}/\Gamma^\circ v^{1/2})_{max}$ were convertible into λ and ψ_{max} respectively according to

$$\log(\lambda) = \log(0.5 + n_i) + \log\{l\sqrt{k_{spr}/2RT}\}$$

and

$$\log(\psi_{max}) = \log\left\{\left(\frac{i_{pa}}{\Gamma^\circ\sqrt{v}}\right)_{max}\right\} - \log\left\{\frac{FS}{RT}\sqrt{\frac{2Fk_{spr}D}{\pi}}\right\}$$

It would require the knowledge of the global parameters $k_{spr}D$ and $l\ k_{spr}^{1/2}$. The use of logarithmic plots in Figure 9a helps to circumvent the difficulty since the $\log(\psi_{max})$ vs $\log(\lambda)$ and $\log(i_{pa}/\Gamma^\circ v^{1/2})_{max}$ vs $\log(x_e)$ curves have similar slopes. Both are almost linear at high λ (or x_e) and take a characteristic turn as λ (or x_e) decreases. These common features must superpose and only narrow ranges of $k_{spr}D$ and $l\ k_{spr}^{1/2}$ values are available for the adjustment of the computed curve to the experimental data. The best fit, shown in Figure 9a, is obtained for $k_{spr}D = 2.2 \times 10^8$ W/mol and $lk_{spr}^{1/2} = 89$ (J/mol)$^{1/2}$.

The other striking feature is the very characteristic shift of the peak potentials with $\log(v)$ plotted in Figure 4b. Quantitatively, the critical potential scan rate defined as v_c in Figure 4b is expected to correspond to the equivalent dimensionless parameter β_c (Figure 8b). The variation of v_c with x_e is therefore expected to resemble the variation of β_c with λ. Adjusting the theoretical and experimental variations unequivocally would require again the knowledge of $k_{spr}D$ and $l\ k_{spr}^{1/2}$. For the same reasons as described above for the fitting of $\log(i_{pa}/\Gamma^\circ v^{1/2})_{max}$ vs $\log(x_e)$, the common characteristic features of the logarithmic plots can be used to obtain a satisfactorily accurate adjustment of the computed $\log(\beta_c)$ vs $\log(\lambda)$ curve to the experimental data, $\log(v_c)$ vs $\log(x_e)$, as shown in Figure 9b. The values of $k_{spr}D = 1.7 \times 10^8$ W/mol and $l\ k_{spr}^{1/2} = 97$ (J/mol)$^{1/2}$ thus obtained are in very good agreement with those of the same parameters derived independently from the measurement of peak currents.

Adsorption of whole IgG's or Fab fragments at glassy carbon electrodes gives in both cases a surface concentration of $\sim 10^{-12}$ mol/cm^2; thus, the lateral distance separating two adsorbed entities is larger in the case of adsorbed Fab fragments. Another major difference is that each adsorbed IgG can be recognized by more than one antibody (or Fab) molecule whereas each adsorbed Fab can be recognized by only one antibody.[5e] As a result, the average distance at which the whole antibodies of the second monolayer are located is expected to be smaller in the case of a construction starting with adsorbed Fab fragments. That is why the value 0.5 is ascribed to n_i in Figure 3a. In that case, the exact value of n_i does not actually matter since the point ascribed to $n_i = 0.5$ lies in the horizontal part of the fitting curves in Figure 9. However, when the self-assembly consisted of the adsorbed goat Fab/anti-goat IgG/Fc-labeled anti-goat IgG sequence of successively immobilized monolayers, we observed that $(i_{pa}/\Gamma^\circ v^{1/2})_{max}$ was higher than in the case of construction 3c, indicating that the distance x_e was lower. Thus the value of $n_i = 1.25$ was ascribed to the corresponding construction.

The combination of the two global parameters $k_{spr}D = (2 \pm 0.5) \times 10^8$ W/mol and $l\ k_{spr}^{1/2} = (93 \pm 5)$ (J/mol)$^{1/2}$ yields $l/D^{1/2} = (0.7 \pm 0.2) \times 10^{-2}$ s$^{-1/2}$ in remarkably good agreement with the value of the equivalent parameter determined for Fc−PEG chains diffusing freely through the IgG self-assembly assimilated to a membrane $l/(D_m)^{1/2} = (1 \pm 0.2) \times 10^{-2}$ s$^{1/2}$.[6] The distance l lies between 0.5 and 1 times the IgG size of 15 nm.[10] Then $10^{-8} \leq D \leq 4.6 \times 10^{-8}$ cm^2/s and $0.4 \times 10^{11} \leq k_{spr} \leq 1.5 \times 10^{11}$ pN/mol·nm. That leads to $0.07 \leq k^\circ_{spr} \leq 0.25$ pN/nm for the spring constant k°_{spr} of a single-chain molecule. The chain spring constant of a polymer in a good solvent is estimated as

$k°_{spr} = 3k_BT/R_F^2$.[12] The Flory radius of the PEG−Fc chain we attached being $R_F = 5$ nm, that would give $k°_{spr} = 0.5$ pN/nm. The reasonable agreement between the latter value and the value we derive from our measurements is rather comforting. However, it should be kept in mind that the step-by-step construction presently described does not produce an ideal array of chains all located at the same distance from the electrode surface. It rather consists of numerous chains grafted all around the bulky Fc−PEG−IgG's which were self-assembled at the top of the IgG structure. Only the average behavior of the chains distribution is experimentally observed. Nevertheless, a detailed quantitative analysis of the voltammetric transient response provides clear evidence that the experimentally observed behavior can be justified and predicted according to the model of elastic bounded diffusion we elaborated. In that context, the values of D or k_{spr} derived above appear quite reasonable.

It is also worth underlining that the experimentally observed behavior can be very satisfactorily described without taking into account the rate of heterogeneous electron transfer and/or the rate of electron hopping between the ferrocene heads. The absence of control by the former of these two phenomena results from the fact that bounded diffusion causes the mass transfer to be always slower than the heterogeneous electron transfer. That electron hopping does not interfere is ascertained experimentally by the independence of the characteristics of the cyclic voltammograms on the Fc head coverage. The Fc head coverage was altered in two different ways either by simultaneous self-assembly of mixtures of Fc−PEG−IgG's and unlabeled IgG's within the same monolayer or by immobilization of Fc−PEG−IgG's bearing markedly different numbers of PEG−Fc chains. Moreover, the Fc volume concentration is typically located in the 5−10 mM range. That corresponds to an extremely low fractional coverage as defined in ref 7, and no significant kinetic control by electron hopping is expected.

Experimental Section

Chemicals. The goat and mouse IgG's (affinity-purified whole molecules) used as sacrificial antigens and the polyclonal anti-goat mouse IgG (affinity-purified whole molecules) were from Jackson laboratories. The polyclonal anti-mouse goat IgG (affinity-purified whole molecules) was a Rockland product. All the IgG molar weights were ~150 000. The Fab fragment of polyclonal anti-mouse goat antibody was from Biosys (Compiègne, France). The ferrocene, *N*-hydroxysuccinimide activated ester, heterodisubstituted poly(ethylene glycol) linear chain of 3400 average molar weight (NHS−PEG−Fc) was synthesized and characterized as previously described.[1c] All other chemicals were purchased from Aldrich. They were used as received. The PBS buffer was made of 0.01 M KH_2PO_4 and 0.15 M NaCl, pH being adjusted to 7.4 with a 1 M NaOH solution; 0.1% sodium azide was added when the buffer was used for storage. Unless otherwise specified, all the protein-containing solutions were prepared in PBS buffer. Centricon-30 was purchased from Amicon.

Cyclic Voltammetry. The instrumental setup was the same as previously described.[14] The temperature in all experiments was 25 °C. All solutions were purged from dioxygen before each voltammetric run. Provided that prolonged overcompensation was avoided, the IgG assemblies did not suffer from the use of the ohmic drop compensation feedback loop. Thus, reliable ohmic-drop-free cyclic voltammograms could be recorded even at the highest potential scan rates. All potentials are referred to the KCl-saturated calomel electrode (SCE).

Attachment of PEG−Fc Chains to Mouse Anti-Goat and Goat Anti-Mouse IgG's. The reaction of the NHS activated ester with amino groups of the IgG species was adapted from the literature[3] and carried out as follows: 2.3 mM NHS−PEG−Fc (MW = 3400) and 2.5 mg/mL affinity purified IgG were allowed to react for 4 h in 145 μL of pH 8 phosphate buffer (0.1 M ionic strength) in the dark at room temperature. It corresponds roughly to a Fc−PEG−NHS/IgG ratio of 140. The IgG's were separated from unattached Fc−PEG chains by ultrafiltration through a Centricon 30 YM cellulose membrane. The membrane is permeable to the PEG chains (MW ≤ 5000), and it retains the IgG molecules which are thus concentrated in the residual solution.[15] After five concentration/dilution cycles, corresponding to a total dilution factor of 10^6 for the unattached PEG chains, PBS buffer containing 0.01% sodium azide was added to the residual solution to reach a total volume of 0.5 mL. The solution thus obtained, containing ~0.7 mg/mL labeled IgG, was stored in a refrigerator for further use. The iron content, i.e., the Fc content of the solution, was assayed by ICP-MS.

Adsorption of the First Monolayer of Sacrificial Antigen. The 3-mm-diameter glassy carbon disk electrodes were prepared as described previously.[14] They were successively polished with sand paper and diamond pastes of 3- and 1-μm particle size. The electrodes were ultrasonicated in dichloromethane between each polishing step. Adsorption of goat or mouse IgG was obtained by wetting the electrode surface with a drop of 1 mg/mL IgG solution in PBS buffer. The electrode was then thoroughly rinsed, washed with the buffer, dipped into a 0.1 mg/mL solution of gelatin in PBS for 10 min, and rinsed again. The gelatin treatment was used to prevent the occurrence of nonspecific binding. The electrode was then ready for the antigen−antibody reaction-driven immobilization of the next IgG monolayers.

Step-by-Step Construction of the IgG Multilayer Assembly. Immobilization of a new monolayer of antibody on top of an already immobilized monolayer of antigen was carried out by immersing the modified electrode into the antibody solution. As already shown,[5] an immersion time of 6 h in a 20 μg/mL IgG solution or an overnight immersion in a 10 μg/mL IgG solution is sufficient to ensure the attachment of a saturated monolayer of antibody. The regular step-by-step growth of the multimonolayer assembly was ascertained as follows. Successful immobilization of the new monolayer was checked in blank experiments by letting the corresponding electrode stand in a solution containing a glucose oxidase-labeled antibody to the IgG whose presence was expected in the outermost monolayer. The resulting enzyme coverage was then derived from the measure of its catalytic activity as described previously.[5] When the antigenic nature of the outermost monolayer is such that it can be recognized by the glucose oxidase antibody conjugate, a saturating coverage of the enzyme is detected ($\Gamma_{enz,sat} = 2.9 \times 10^{-12}$ mol/cm^2). When the antigenic nature of the outermost monolayer is not the expected one, a much weaker enzyme coverage resulting solely from nonspecific binding is detected (Γ_{enz} markedly below 10^{-12} mol/cm^2). Immobilization of the Fc−PEG−IgG layer was carried out by immersing the electrode covered with the appropriate assembly into a 15 μg/mL solution of Fc−PEG−IgG for 48 h. The modified electrodes were stored in the dark, at room temperature in PBS plus sodium azide buffer.

Conclusion

The model of elastic bounded diffusion we elaborated for the quantitative analysis of the dynamics of probes borne by the loose ends of linear and flexible polymeric chains terminally grafted to building blocks of a self-assembled construction describes very satisfactorily the experimentally observed behavior. The creation of an oriented concentration gradient provokes a diffusion-like displacement of the probes which is counterbalanced by a springlike elastic penalty. The transient excitation and measurement technique used in the present study is cyclic voltammetry. The construction, immobilized at a glassy carbon electrode surface, is made of successively self-assembled monolayers of immunoglobulins. A ferrocene redox probe is attached at the loose end of a flexible poly(ethylene glycol) chain. Depending on the distance x_e at which the PEG chains are grafted and/or on the potential scan rate, the cyclic

(14) Bourdillon, C.; Demaille, C.; Moiroux, J.; Savéant, J.-M. *J. Am. Chem. Soc.* **1993**, *115*, 2−10.

(15) Karr, L. J.; Donnelly, D. L.; Kozlowski, A.; Harris, J. M. *Methods Enzymol.* **1994**, *228*, 377.

voltammograms exhibit quite characteristic features. Particularly the morphology and the intensity of the signal may change dramatically. The observed changes are qualitatively and quantitatively justified by the model. That gives access to the two parameters characterizing diffusion of the ferrocene heads within the self-assembled IgG structure on the one hand and the elasticity of the PEG chains on the other. The diffusion coefficient is the same as the one found for free diffusion of unattached PEG chains through the structure. The apparent spring constant is in satisfactory agreement with the one predicted in the literature for the PEG chain in its random coil conformation.

Acknowledgment. We are indebted to Prof. J. L. Colin for the ICP-MS iron assays.

Supporting Information Available: Elastic bounded diffusion: solution of set (3) of differential equations. This material is available free of charge via the Internet at http:/pubs.acs.org."

JA991780I